

# The Importance of the Pressure Anisotropy Induced by Strong Magnetic Fields on Neutron Star Physics

**Efrain J Ferrer and Aric Hackebill**

Dept. of Physics and Astronomy, University of Texas Rio Grande Valley, Edinburg 78539, USA ; Dept. of Physics and Astronomy, CUNY-Gerad Center, New York 10314, USA

E-mail: [efrain.ferrer@utrgv.edu](mailto:efrain.ferrer@utrgv.edu), [ahackebill@gradcenter.cuny.edu](mailto:ahackebill@gradcenter.cuny.edu)

**Abstract.** In this paper we discuss in some detail how the pressures determined from semi-classical statistical averaging of the energy momentum tensor in the presence of a uniform background magnetic field are anisotropic with different pressures arising along and perpendicular to the magnetic field direction. Hence, we analyze how this result can affect two important characteristics of dense magnetized systems: (i) The hadron-quark phase transition in the presence of a magnetic field, (ii) The behavior of the speed of sound in dense magnetized systems. Taking into account that large magnetic fields are expected to be present in the interior of neutron stars, we will stress the role the pressure anisotropy plays in the physics of these compact astronomical objects.

## 1. Introduction

There are many studies in the literature that analyze the behavior of the first-order quark-hadron phase transition in the presence of a magnetic field [1, 2]. All of these studies were done using isotropic Maxwell or Gibbs equilibrium conditions, where the pressures in the two phases were considered to be isotropic. However, it was shown in [3, 4] that in a system of charged fermions immersed in a background magnetic field the system's pressures are anisotropic with different pressures arising in the directions parallel to and perpendicular to the field direction. In [5] the study of the pressure anisotropy was extended to neutral composite particles (neutrons), where the particles were taken to interact with the magnetic field through their anomalous magnetic moments (AMM). Since neutron stars (NS) are known to have strong surface magnetic fields, with magnetars having surface fields as large as  $10^{14}$ - $10^{16}$ G [6], and potentially even larger interior fields, with estimates as high as  $10^{18}$ G [7] for hadrons and  $10^{20}$ G for quarks [4], it is important to understand the significance of the magnetic field induced pressure anisotropy on NS physics. In what follows we give an overview of the potential significance of the pressure anisotropy in the context NS and pinpoint some key, model-dependent features of the anisotropy that are important to take into consideration when modeling NS matter.

## 2. The Magnetic Field Induced Anisotropy of the Equation of State

In this section we offer a pedagogical overview of the analysis of the magnetic field induced anisotropy in the equation of state (EOS), which was introduced in [4] for a charged fermion system in a background magnetic field. The main idea is to determine the stress energy tensor (SET) semi-classically by taking the quantum-statistical average of the components of the



Content from this work may be used under the terms of the [Creative Commons Attribution 3.0 licence](https://creativecommons.org/licenses/by/3.0/). Any further distribution of this work must maintain attribution to the author(s) and the title of the work, journal citation and DOI.

symmetrized field-theoretic energy momentum tensor. In this way the EOS can be determined from the system's pressures and energy density, which are realized as the diagonal components of the semi-classical SET.

### 2.1. Symmetries of a magnetized system

Although the magnetic field induced anisotropy in the EOS can be derived directly from a semi-classical calculation, it may be helpful to note that the anisotropy might be expected to be present from pure symmetry considerations. The symmetries of a magnetized matter system can be expressed through three independent structures in the SET

$$T^{\mu\nu} = a_1 \eta^{\mu\nu} + a_2 u^\mu u^\nu + a_3 \hat{F}^{\mu\rho} \hat{F}_\rho^\nu, \quad (1)$$

where  $\eta^{\mu\nu}$  is the Minkowski metric,  $u_\mu$  is the medium four-velocity, which in the rest frame takes the form  $u_\mu = (1, \vec{0})$ ,  $\hat{F}^{\mu\rho} = F^{\mu\rho}/B$  is the normalized field strength tensor, and  $a_i$ ,  $i = 1, 2, 3$  are scalar coefficients. A system devoid of matter and electromagnetic fields is locally characterized by complete Lorentz symmetry, which is reflected in (1) by taking  $a_2 = a_3 = 0$ . Under these conditions the only available structure is the local spacetime structure, which is described by  $\eta^{\mu\nu}$ . Once a medium is included, the local  $SO(1,3)$  symmetry is broken by the introduction of a preferred direction that is locally aligned with the medium's four velocity. This corresponds to the case where  $a_3 = 0$ , which is concordant with the familiar form of the SET for a perfect fluid. At this point,  $O(3)$  symmetry is still present for frames comoving with the fluid, but once a uniform background magnetic field is introduced the  $O(3)$  symmetry is broken by a new preferred direction that is locally aligned with the field. The third term in (1), which was originally derived in [4], is included to reflect this further symmetry breaking. Note that in a local basis where the magnetic field is aligned with the  $\hat{z}$  direction,  $diag(\hat{F}^{\mu\rho} \hat{F}_\rho^\nu) = (0, -1, -1, 0)$ , which is concordant with the intuition that there should now be an asymmetry in the SET between the components along and perpendicular to the local magnetic field direction. It then remains to perform the semi-classical calculation in order to determine the coefficients  $a_i$  and to check that (1) indeed expresses the correct form of the SET.

### 2.2. Determining the semi-classical SET through quantum statistical averaging

Following considerations made in ([8], Sec. 3.4), the semi-classical SET can be determined in the context of NS by considering a volume element of the star that is small enough so that the magnetic field is approximately uniform throughout it and so that general relativistic effects may be ignored, but large enough so that the element contains enough statistical degrees of freedom, e.g. particles, lattice sites, etc., to make statistical calculations meaningful. Quantum statistical averaging of the field theoretic energy momentum tensor, which describes the microphysics on the volume element, then determines the semi-classical SET as follows

$$T^{\mu\nu} = \frac{1}{\beta V} \frac{\text{Tr}[\hat{\tau}^{\mu\nu} e^{-\beta(\hat{H}-\mu\hat{N})}]}{\mathcal{Z}}, \quad (2)$$

where  $\beta = \frac{1}{T}$  is the inverse absolute temperature of the system,  $V$  is the volume of the volume element,  $\hat{H}$  is the Hamiltonian,  $\hat{N}$  is the particle number operator,  $\mu$  is the chemical potential,  $\hat{\tau}^{\mu\nu} = \int_0^\beta d\tau \int_V dx^3 \hat{\tau}^{\mu\nu}$  is the integral of the energy momentum tensor operator  $\hat{\tau}^{\mu\nu}$  over the system's Euclidean spacetime region, and  $\mathcal{Z}$  is the partition function of the grand canonical ensemble, which is given by

$$\mathcal{Z} = \text{Tr}[e^{-\beta(\hat{H}-\mu\hat{N})}]. \quad (3)$$

In [4], path integral techniques were used to compute (2) for a dense, charged fermion system in a background magnetic field directed along the  $\hat{z}$  direction to arrive at

$$T^{\mu\nu} = \Omega\eta^{\mu\nu} + (\mu\rho + TS)u^\mu u^\nu + BM\eta_\perp^{\mu\nu}, \quad (4)$$

where  $\Omega$  is the system thermodynamic potential,  $\rho = -(\partial\Omega/\partial\mu)_{V,T}$  is the average particle-number density,  $S = -(\partial\Omega/\partial T)_{V,\mu}$  is the entropy density,  $M = -(\partial\Omega/\partial B)_{V,T,\mu}$  is the system magnetization,  $V$  is the system volume, and  $B$  is the magnetic field. Notice that the result of the quantum statistical averaging (4) is in agreement with (1), with  $a_1 = \Omega$ ,  $a_2 = (\mu\rho + TS)$ , and  $a_3 = BM$ .

### 2.3. The Anisotropic EOS at $T = 0$

If we consider the case of a old, cold star where  $\mu \gg T$  and the  $T \approx 0$  approximation is appropriate, then in a frame comoving with the stellar medium, (4) has the following diagonal components

$$\varepsilon = T^{00} = \Omega - \mu\rho + \frac{B^2}{2}, \quad (5)$$

$$P_\perp = T^{11} = T^{22} = -\Omega - MB + \frac{B^2}{2}, \quad (6)$$

$$P_\parallel = T^{33} = -\Omega - \frac{B^2}{2}, \quad (7)$$

where  $\varepsilon$  is the system's energy density,  $P_\perp$  is the system's pressure along the direction perpendicular to the field direction, and  $P_\parallel$  is the system's pressure along the field direction. The system's pressures are clearly anisotropic, with the anisotropy manifesting in two important ways: (i) through a difference in sign between the so called "Maxwell terms" arising from the pure electromagnetic contribution to the SET that are quadratic in the field and (ii) through the presence of the magnetization term in the pressures perpendicular to the field direction.

### 2.4. Ongoing discussion of the pressure anisotropy

We would like to point out that there is an ongoing discussion of the existence and nature of the pressure anisotropy. Majority of the discussion has been focused on whether or not the magnetization term, seen in (6), is present in systems of interest. In this regard, it was originally conjectured in [9] that the magnetization term is cancelled out by a similar term resulting from the Lorentz force induced by the system's self-magnetization. Further arguments for this position were made in [10] and some counterarguments were made in [11, 12], where it is argued that any counter-terms appearing in the SET should be derived in a self consistent way from a microphysical model. We should also say that in [13], the magnetization term is shown not to appear in the hydrodynamic equations, which is given by the vanishing divergence of the SET, when magnetic field generating currents determined from reasonable symmetry considerations are included in the SET. Since the pressures of the system are given by the spatial diagonal components of the SET, and not by its divergence, we believe that the pressures are not subject to the same cancellation that occurs in the hydrodynamic equations. Finally, even if the discussion of the relevance of the magnetization term is set aside for the moment, there is still the issue of the anisotropy arising from the quadratic terms in (6) and (7), which at strong magnetic fields may provide a significant contribution to the pressure anisotropy. Given this, we believe that the pressure anisotropy is likely present in magnetized fermion systems and its significance on NS physics should be checked.

### 3. The Anisotropic First-Order Phase Transition

In this section we provide a brief overview of the techniques developed in [14] for dealing with phase transitions between magnetized systems where the pressure anisotropy is present. The analysis that follows will be in principle applicable to various phase constructions, e.g. the Maxwell construction (MC), the Gibbs construction (GC), etc., but for the purposes of providing an illustrative example we will focus on the MC for modeling first-order phase transitions, which for isotropic pressures, is characterized by four equilibrium conditions:

$$P^A = P^B, \quad \mu_b^A = \mu_b^B, \quad \sum_i q_i^A = 0, \quad \sum_i q_i^B = 0. \quad (8)$$

Here  $A$  and  $B$  denote the different phases,  $P^{A/B}$  is the pressure in phase  $A/B$ ,  $\mu_b^{A/B}$  is the baryonic chemical potential in phase  $A/B$ , and  $q_i^{A/B}$  are any charges that may be present in each phase. Since the MC requires each phase to be separately charge neutral, each phase has an associated electric chemical potential  $\mu_e^{A/B}$ , which are in principle different in value. Formulated this way, each phase only has one pressure, which arises from the fact that an isotropic pressure assumption is made when the equilibrium conditions in (8) are derived from first principles. Then to see how the MC should be modified to handle anisotropic pressures, we must track down where the isotropic pressure assumption is made in the derivation and determine how it should be modified to accommodate anisotropic pressures.

#### 3.1. The anisotropic mechanical equilibrium condition

Derivations for the pressure equality relation in (8) typically start by considering an isolated system of fixed volume  $V$  that is divided into two subsystems containing phase A and phase B respectively, which are allowed to exchange volume and energy. The variation of the entropy of the total system is given by

$$dS = dS^A + dS^B. \quad (9)$$

Then by introducing the thermodynamic relations:  $dS = dQ/T$ ,  $dE = dQ - dW$ , and  $dW = PdV$  into (9), assuming that  $dQ^A = -dQ^B$ ,  $dV^A = -dV^B$ , and that  $T^A = T^B$  at equilibrium, the variation of the total entropy becomes

$$dS = \frac{1}{T} (P^A - P^B) dV^A. \quad (10)$$

Finally, it is argued that at equilibrium a first differential of the entropy must vanish, which combined with (10) gives the isotropic mechanical equilibrium condition

$$P^A = P^B. \quad (11)$$

Then it is clear that between (9) and (10) the isotropic pressure assumption enters through the assumption that the pressure doing work on a system is isotropic. However, for a system being compressed by anisotropic pressures the work relation must be generalized to

$$dW = P_{\parallel} dV_{\parallel} + P_{\perp} dV_{\perp}, \quad (12)$$

where  $dV_{\parallel}$  is the differential volume change occurring from compression in a particular direction (call it the parallel direction) and  $dV_{\perp}$  is the differential volume change in the direction perpendicular to the parallel direction. Following the derivation between (9) and (10), using the anisotropic work expression (12), and taking into account that  $dV_{\parallel}$  and  $dV_{\perp}$  are independent variations, we arrive at the anisotropic mechanical equilibrium condition

$$P_{\parallel}^A = P_{\parallel}^B, \quad P_{\perp}^A = P_{\perp}^B, \quad (13)$$

which should replace the isotropic pressure condition in (8), to give the equilibrium equations for the anisotropic MC:

$$P_{\parallel}^A = P_{\parallel}^B, \quad P_{\perp}^A = P_{\perp}^B, \quad \mu_b^A = \mu_b^B, \quad \sum_i q_i^A = 0, \quad \sum_i q_i^B = 0. \quad (14)$$

### 3.2. Discontinuity of the magnetic field during first-order phase transitions

The MC for the first-order phase change between two systems  $A$  and  $B$  imposes the anisotropic mechanical equilibrium condition (13), which for magnetized fermion systems where the pressures are described by (6) and (7), takes the explicit form

$$-\Omega_A - \frac{B_A^2}{2} = -\Omega_B - \frac{B_B^2}{2}, \quad (15)$$

$$-\Omega_A - M_A B_A + \frac{B_A^2}{2} = -\Omega_B - M_B B_B + \frac{B_B^2}{2}. \quad (16)$$

If  $B_A = B_B$ , then (15) and (16) together imply that  $M_A = M_B$ . However, in a first-order phase transition the magnetizations, which are first-order derivatives of the thermodynamic potential, are not equal. Then by reductio  $B_A \neq B_B$  for magnetized fermion systems undergoing a first-order phase change. The discontinuity at the phase boundary indicates that the divergence of the magnetic field at the boundary is nonvanishing, which further implies the presence of a surface magnetic charge. An explanation for the surface charge as an accumulation of magnetic monopoles at the interface between the two phases is discussed more thoroughly in [14].

## 4. Magnetic Field Effects on the EOS during a Phase Transition

To study the effects of a magnetic field on the anisotropic quark-hadron phase change explicitly, we consider such a phase change modeled by the MC (14) in a background magnetic field, where the two-flavor quark phase (QP), including electrons, is described by the MIT Bag model [15] and the hadron phase (HP), comprised of neutrons, protons and electrons, is described by the Nonlinear-Walecka (NWL) model. The systems are considered to be beta-equilibrated and at zero temperature. The thermodynamic potentials, EOS, as well as all the parameters contained in those models under these conditions are thoroughly studied and specified in [14]. We refer the reader there for a more detailed treatment. We only point out two components of that study that are relevant here. First, the magnetic field-anomalous magnetic moment (B-AMM) interaction is only included in the HP for the neutrons. This is because the B-AMM interaction was found in [16] to have an insignificant influence on the pressures of charged fermion systems and in [17] to have a significant influence on the neutron component of the pressure at magnetic fields near  $10^{18}$ G, which is the maximum magnetic field strength considered in this section. Second, we point out that the calculations done in [14] were done in the weak-field approximation (WFA), where it was found that the baryonic chemical potential was large enough to justify using the WFA up to field strengths of  $10^{18}$ G. Using the models developed in [14] and fixing the  $B^{HP}$ , the anisotropic equilibrium conditions (14) can be numerically solved to determine all the parameters of the system.

### 4.1. Discontinuity in the magnetization

As discussed in Sec. 3.2, we expect that the first-order phase transition modeled by the anisotropic MC will impose a discontinuity in both the magnetization and the magnetic field

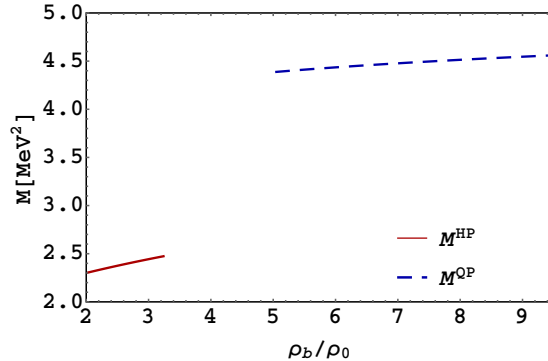


**Figure 1.** (Color online) Magnetization,  $M$ , in the HP (red-solid) and QP (blue-dashed) versus baryonic charge density,  $\rho_b$  normalized against the baryonic saturation density  $\rho_0 = 0.153 \text{ fm}^{-3}$ , at  $B^{\text{HP}} = 10^{16} \text{ G}$ .

between the two phases. The jump in the magnetization can be seen in Fig. 1, where the magnetization of the HP (lower left-hand corner) increases with baryon density until around 3.2 times the baryonic saturation density. There is then a jump in both the baryon density and the magnetization before the QP (upper right-hand corner) begins. Both the jump in the baryon density and the magnetization are compatible with the first-order nature of the phase transition, since both are first derivatives of the thermodynamic potential. What's more, the magnetic field also jumps between the two phases with  $B^{\text{HP}} = 10^{16} \text{ G}$  and  $B^{\text{QP}} - B^{\text{HP}} \text{ G} \approx 4.1 \times 10^{13} \text{ G}$ .

#### 4.2. Behavior of the EOS at strong magnetic fields

In Fig. 2, the behavior of the parallel and perpendicular EOS across a wide range of strong magnetic field values can be seen and the effect of the AMM can be compared. Similar to the behavior of the magnetization, the EOS increases in the HP (lower left-hand corner) before jumping in energy density to the QP (upper right hand corner). It is important to notice that the behavior of the EOS at  $10^{16} \text{ G}$  (black-solid) before and after the phase transition is the same for both the parallel and perpendicular pressures. However, at  $10^{18} \text{ G}$  the parallel pressure shifts down significantly while the perpendicular pressure shifts up. The cause of the shift can be determined from (6) and (7). Since the magnetizations (as seen in Fig. 1) and magnetic fields of both phases are positive, both magnetization terms in (6) are contributing negatively to the pressure. However, the pure Maxwell, quadratic terms are opposite in sign between (6) and (7) and are therefore primarily responsible for the shifting in the EOS. It should be noted though that although the overall direction in shift of the EOS is determined by the Maxwell terms, the magnetization terms in (6) are likely still exerting some influence, which can be seen by the fact that the upward shift in Fig. 2 of the perpendicular pressure is less pronounced than the downward shift in the parallel pressure. This is explained by the fact that the negative contribution of the magnetization term combines with the negative contribution of the Maxwell term in the case of the parallel pressure and partially cancels in the case of the perpendicular pressure where the Maxwell term is positive. Finally, the EOS behave very similarly with or without the AMM even at  $10^{18} \text{ G}$ . The reason for this can be seen by considering the neutron component of the pressure displayed in Fig. 3. The AMM can be seen to significantly effect the parallel pressure after  $10^{18} \text{ G}$  when comparing the bare (no AMM and no Maxwell term) pressure (red-dotted) with the case where the AMM is included (blue-dashed). However, once the Maxwell term is included (black-solid) the parallel pressure begins to decrease profoundly shortly after  $10^{17} \text{ G}$ , completely swamping the effect of the AMM.

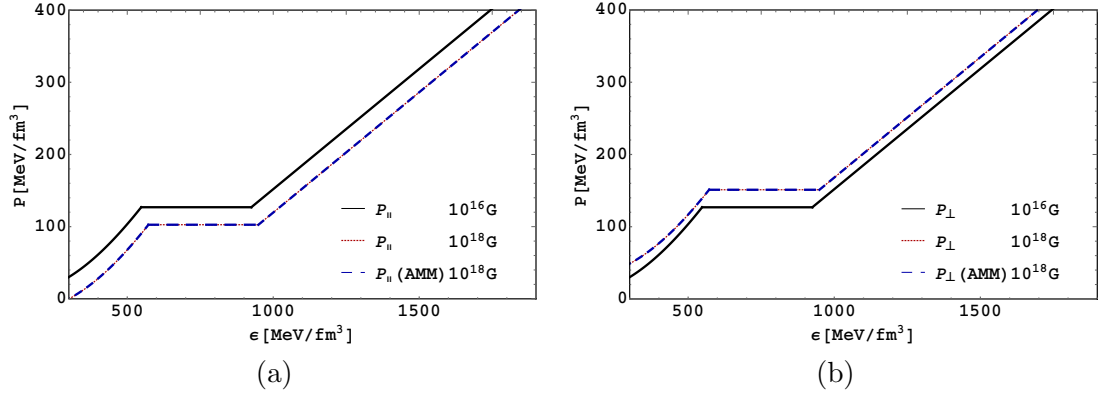


**Figure 2.** (Color online) Parallel (a) and perpendicular (b) EOS in the MC including (blue-dashed) the neutron AMM at  $B^H = 10^{18}$  G and excluding the neutron AMM at  $B^H = 10^{18}$  G (red-dotted) and at  $B^H = 10^{16}$  G (black-solid).

## 5. The Effects of Strong Magnetic Fields on the SOS

In this section we set aside the issue of the quark-hadron phase transition and focus on the effects of the magnetic field induced anisotropy on a system's speed of sound (SOS). In [18], the SOS<sup>2</sup>, which for isotropic systems is defined as the derivative of the pressure with respect to the energy density, was derived for anisotropic, magnetized systems by considering only first-order perturbations in the vanishing divergence of (4). Analogous to the isotropic case, a set of parallel and perpendicular SOS<sup>2</sup> were found to be given by

$$(c_s^{\perp})^2 = \frac{\partial P_{\perp}}{\partial \mu} / \frac{\partial \epsilon}{\partial \mu} = \left[ \frac{\partial P_{\perp}}{\partial \epsilon} \right]_B, \quad (c_s^{\parallel})^2 = \frac{\partial P_{\parallel}}{\partial \mu} / \frac{\partial \epsilon}{\partial \mu} = \left[ \frac{\partial P_{\parallel}}{\partial \epsilon} \right]_B. \quad (17)$$

In the previous section it was shown that for the models considered there, the EOS was primarily influenced through the Maxwell terms. Since (17) is defined through derivatives with respect to the chemical potential, the influence of the Maxwell terms are eliminated from the SOS. It is then of interest to determine what effects the system's anisotropy can have on the SOS.

### 5.1. The MDCDW phase

We now consider the MDCDW phase [19, 20], in which the quarks, described by the mean-field NJL model, form an inhomogeneous chiral condensate characterized by two parameters: the condensate magnitude  $m$  and modulation  $q = b/2$  and having the following scalar and pseudoscalar components

$$\langle \bar{\psi} \psi \rangle = m \cos q_{\mu} x^{\mu}, \quad \langle \bar{\psi} i \tau^3 \gamma^5 \psi \rangle = m \sin q_{\mu} x^{\mu}, \quad (18)$$

where the modulation is taking along the field direction,  $q^{\mu} = (0, 0, 0, q)$ , since this configuration minimizes the system energy [19]. The medium component of the zero-temperature thermodynamic potential for quark flavor  $f$  was determined in [21] to be

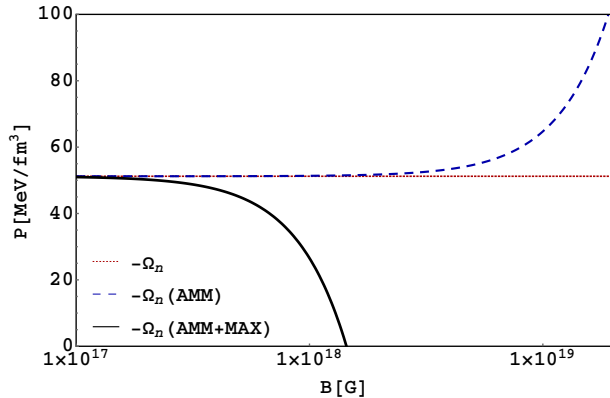


**Figure 3.** (Color online) Neutron component of the parallel pressure without the AMM and Maxwell term (red-dotted), with the AMM, but without the Maxwell term (blue-dashed), and with both the AMM and Maxwell term (black-solid) as a function of the magnetic field.

$$\begin{aligned} \Omega_f^{med} = & -\frac{|e_f B|}{(2\pi)^2} \mu_f q - \frac{|e_f B|}{8\pi^2} \int_{-\infty}^{\infty} dp_3 \sum_{\epsilon \in \{+,-\}} (|E_{0,\epsilon} - \mu_f| - |E_{0,\epsilon}|) \Big|_{reg} \\ & - \frac{|e_f B|}{(2\pi)^2} \int_{-\infty}^{\infty} dp_3 \sum_{l>0, \xi \in \{+,-\}} \left( \mu_f - E_{l,\xi,\epsilon}^f \right) \Theta \left( \mu_f - E_{l,\xi,\epsilon}^f \right) \Big|_{\epsilon=+}, \end{aligned} \quad (19)$$

where the energy spectra are given by

$$\begin{aligned} E_{0,\epsilon} &= \epsilon \sqrt{m^2 + p^2} + b, \quad \epsilon = \pm, l = 0 \\ E_{l,\xi,\epsilon}^f &= \epsilon \left[ \left( \xi \sqrt{m^2 + p^2} + b \right)^2 + 2|e_f B|l \right]^{1/2}, \quad \epsilon = \pm, \xi = \pm, l = 1, 2, 3, \dots \end{aligned} \quad (20)$$

The so called "anomalous" first term in (19) is then of relevance to the anisotropic SOS for two reasons. First, it couples  $B$  with  $\mu_f$ , thus making the magnetization through that term proportional with  $\mu_f$ . Since the chemical potential is typically the largest parameter in NS physics, it suggests that there may be a large anisotropy in the system that is generated by the magnetization term in (6). Second, the coupling of  $B$  and  $\mu_f$  also suggests through (17) that SOS may be high at large magnetic field strengths.

### 5.2. Numerical results for the MDCDW phase SOS

We consider a charge-neutral, beta equilibrated, two-flavor magnetized system of quarks and electrons with the quarks modeled by the MDCDW phase (for a detailed description see [18]). For the purposes of modeling hybrid NS at intermediate densities, we take ( $320\text{MeV} \leq \mu_f \leq 340\text{MeV}$ ). Under these conditions  $m \ll \mu_f$  (see Fig. 2 in [22]) and  $m$  can be neglected. Then the SOS<sup>2</sup> of the MDCDW phase under these conditions can be obtained by first determining the MDCDW EOS through plugging (19) into (5), (6) and (7), and then by plugging that result into (17).

In Fig. 4, the behavior of the parallel and perpendicular SOS<sup>2</sup> for this system can be seen. Since the magnetic fields being considered are relatively high, the WFA is not being used here. Rather the full sum over Landau levels (LL) indexed by  $(l)$  in (20) has been performed. This is

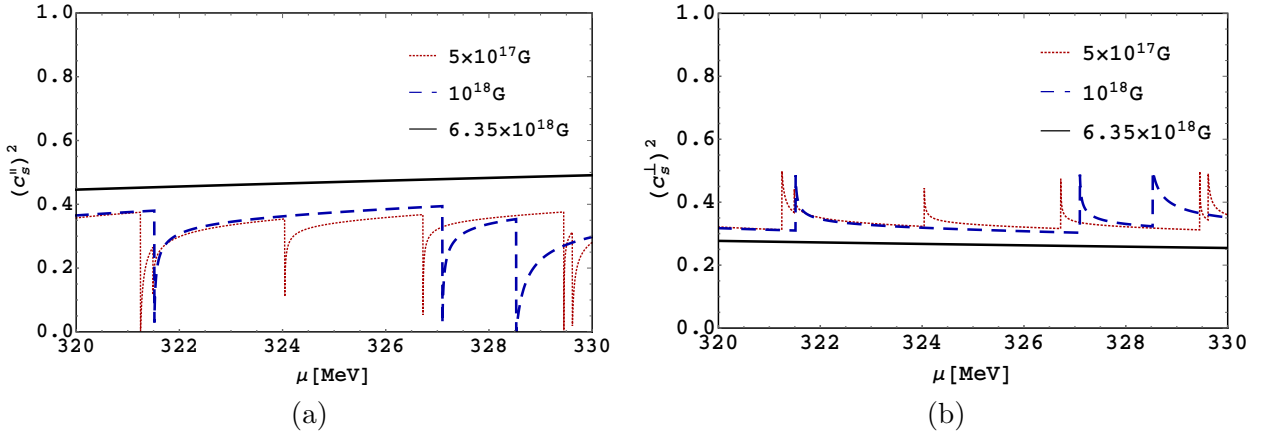


**Figure 4.** (Color online) Parallel (a) and Perpendicular (b)  $SOS^2$  in the MDCDW phase versus baryonic chemical potential corresponding to intermediate densities for different applied magnetic fields.

responsible for the Hass-van Alphen oscillations seen in the  $SOS^2$  at the two lower field values. The maximum term of the Landau sum is  $\mu_f$  dependent and determined by the behavior of the Heaviside function in (20). Then at fixed values of the field, as  $\mu_f$  increases new terms enter the Landau sum, which results in the oscillations. The parallel and perpendicular  $SOS^2$  display markedly different behavior, with the parallel  $SOS^2$  reaching a higher maximum value (roughly  $.5c$ ) than its perpendicular counterpart. This is a merit of the MDCDW phase, since it is known that for hybrid stars where the QP  $SOS^2$  is at or below the conformal limit, i.e.  $c_s^2 \leq 1/3$ , it is impossible to reach stellar masses of  $\sim 2M_\odot$  [23], which are observed in nature. It should also be noted that the parallel  $SOS^2$  in Fig. 4 appears to decrease as the baryonic chemical potential increases for the two lower magnetic fields considered. However, this is a result of the irregular behavior of the Hass-van Alphen oscillations. On a larger domain the parallel  $SOS^2$  exhibits no apparent decrease.

## 6. Conclusions

In this paper we reviewed some important effects that are present in magnetized systems. First we pointed out that the magnetic field induced pressure anisotropy implies a discontinuity in the magnetic field between two phases undergoing a first-order phase transition. We then showed that the Maxwell terms in (6) and (7) are responsible for generating significant anisotropies in the EOS of magnetized systems undergoing a first-order phase change at fields greater than  $10^{17}\text{G}$ . Lastly, we showed that, apart from the Maxwell contributions, the system anisotropy may significantly affect other properties, e.g. the SOS, through the magnetization term in (6) and analyzed the case study of the MDCDW phase, which at high magnetic fields was seen to have  $SOS^2$  exceeding the conformal limit. Pronounced anisotropic effects may then occur at field values close to the upper limit of values applicable to NS.

## References

- [1] Bandyopadhyay D, Chakrabarty S and Pal S, Phys. Rev. Lett. 79 (1997) 2176; Orsaria M, Ranea-Sandoval I F, Vucetich H, Weber F, Int. J. Mod. Phys. E 20 (2011) Supp. 02, 25; Casali R H, Castro L B, Menezes D P, Phys. Rev. C 89 (2014) 015805; Franzon B, Dexheimer V and Schramm S, Mon. Not. Roy. Astron. Soc. 456 (2016) 2937.
- [2] Rabhi A, Pais H, Panda P K and Providencia C, J. Phys. G: Nucl. Part. Phys. 36 (2009) 115204.

- [3] Canuto V and Chiu H Y, Phys. Rev. 173 (1968) 1210.
- [4] Ferrer E J, de la Incera V, Keith J P, Portillo I and Springsteen P L, Phys. Rev. C 82 (2010) 065802.
- [5] Ferrer E J and Hackebill A, Phys. Rev. C 99 (2019) 065803.
- [6] Ibrahim et al., Astrophys. J. 609 (2004) L21; Kulkarni S and Frail D, Nature 365 (1993) 33; Murakami T et al., Nature 368 (1994) 127; Marsden D and Higdon J C, The Astro. Phys. Jour., 550 (2001) 397; Dib R, Kaspi V M, and Gavriil F P, The Astro. Phys. Jour., 673 (2008) 1044.
- [7] Bocquet M, Bonazzola S, Gourgoulhon E, and Novak J, Astron. Astrophys. 301 (1995) 757; Dong L and Shapiro S L, ApJ. 383 (1991) 745.
- [8] Glendenning N K, *Compact Stars*, (2000) New York: Springer.
- [9] Blandford R D and Hernquist L, J. Phys. C 15 (1982) 6233.
- [10] Potekhin and A Y and Yakovlev D G, Phys. Rev. C 85 (2012) 039801.
- [11] Ferrer E J and de la Incera V, Phys. Rev. C 85 (2012) 039802.
- [12] Dexheimer V, Menezes D P and Strickland M, J. Phys. G 41 (2014) 015203.
- [13] Chatterjee D, Elghozi T, Novac J and Oertel M, Mon. Not. Roy. Astron. Soc. 447 (2015) 3785.
- [14] Ferrer E J and Hackebill A, Int. J. Mod. Phys. A 37 (2022) 2250048.
- [15] Chodos A, Jaffe R L, Johnson K, Thorn C B, and Weisskopf V F, Phys. Rev. D 9 (1974) 3471; Paulucci L, Ferrer E J, Horvath J E, de la Incera V, J. Phys. G 40 (2013) 125202.
- [16] Ferrer E J, de la Incera V, Manreza Paret D, Perez Martinez A, and Sanchez A, Phys. Rev. D 91 (2015) 085041.
- [17] Broderick A, Prakash M, and Lattimer J M, Astrophys. J. 537 (2000) 351.
- [18] Ferrer E J, Hackebill A, Nucl. Phys. A 1031 (2023) 122608
- [19] Frolov I E, Zhukovsky V Ch and Klimenko K G, Phys. Rev. D 82 (2010) 076002.
- [20] Ferrer E J and de la Incera V, Phys. Lett. B 769 (2017) 208.
- [21] Ferrer E J and de la Incera V, Phys. Lett. B 769 (2017) 208; Universe 4 (2018) 54.
- [22] Gyory W and de la Incera V, Phys. Rev. D 106 (2022) 016011.
- [23] Bedaque P and Steiner A W, Phys. Rev. Lett., 114 (2015) 031103 (see also the more recent publications: Tews I, Carlson J, Gandolfi S, and Reddy S, Astrophys. J. 860 (2018) 149; Reed B and Horowitz C, Phys. Rev. C, 101 (2020) 045803; Drischler I C, Han S and Reddy S, arXiv: 2110.14896 [nucl-th]).